Asian Journal of Water, Environment and Pollution, Vol. 6, No. 1, pp. 67-80.

Hydrodynamic and Transport Model of the Siak Estuary

Mutiara R. Putri and Thomas Pohlmann[1]

Research Groups of Oceanography, Institute of Technology Bandung, Jalan Ganesha 10, Bandung 40191, Indonesia
[1]Institute of Oceanography, Center for Marine and Atmospheric Research (ZMAW), University of Hamburg
Bundesstr 53, 20146 Hamburg, Germany
✉ mutiara.putri@zmaw.de

Received July 23, 2007; revised and accepted May 21, 2008

Abstract : The Siak River flows around an industrial area of Riau Province, Sumatra (Indonesia) towards the Malacca Strait. Most of domestic and industrial wastes are transported along this river to the estuary. In this investigation, the HAMburg Shelf Ocean Model (HAMSOM) and an attached dispersion model are employed to simulate the circulation patterns and the dispersion of pollutants, respectively. In this study the pollutants are released only in the front of Siak river mouth. The simulation is performed for the period from January 2001 until May 2006, and the results are validated with available observations and satellite data.

By means of this model study, it is shown that although the wind direction changes with the monsoon, the direction of the surface currents in the Malacca Strait are almost the same over the entire year. Results of the transport model suggest that most of the pollutants are transported through the Bengkalis Strait to the north into the Malacca Strait. Although the general circulation pattern in the Malacca Strait does not show a seasonal reversal, it could be demonstrated that the monsoon cycle influences the transport and dispersion of the pollutants significantly.

Key words: Siak, HAMSOM, Malacca, waste.

Introduction

Riau Province is located in the east of Sumatra and has an extended coastal zone including a number of large and small islands along the coast of the Malacca Strait. This province covers an area of 329,867.61 km^2, from which 71% consists of ocean. There are about 15 rivers in the province with four of them being more important and used as waterways, namely, the Siak river with 8-12 m depth and 300 km length, the Rokan river with 6-8 m depth and 400 km length, the Kampar river with about 6 m depth and 400 km length, and the Indragiri river with 6-8 m depth and 500 km length. The headwaters of these rivers are located in the Bukit Barisan Mountain, in the western part of Sumatra. All of these rivers release their water into the Malacca or Karimata Strait.

As one of Indonesia's richest province with oil, gas, agriculture and plantation resources, the development in this province is very fast as well as the population growth. The population in Riau Province amounts to 5,281,000, with more than 50% of them living on the small islands and more than 580, 000 people living in Pakanbaru city (Bureau of Statistics of Riau Province (BPS Riau), 2000).

Pakanbaru is the capital city of Riau Province from where the Siak River flows another 100 km to the northeast before it enters the Bengkalis Strait. There are a number of factories and urban and rural households along the river discharging waste into the river directly which leads to the fact that the Siak River is one of the strongly polluted rivers in Indonesia. Closer to the estuary, the pollutant concentrations increase and the type of the pollutants are getting more diverse. This contamination of the estuary has a negative impact on public health, which used the Siak River water and the chemical and biological system including the biodiversity (Nedi, 1999).

Because of the shallow water depth and the large number of small islands around the Malacca Strait, the energy input from ocean current and waves into the Siak estuary is significantly reduced. By this means the islands and straits around the Siak river estuary also suppress the transport of pollutant from the Siak estuary into the Malacca Strait (Figure 1). However, the periodicity of tides in combination with the effect of the shallow water depth strongly tends to cause vertically homogeneous conditions in the Riau waters.

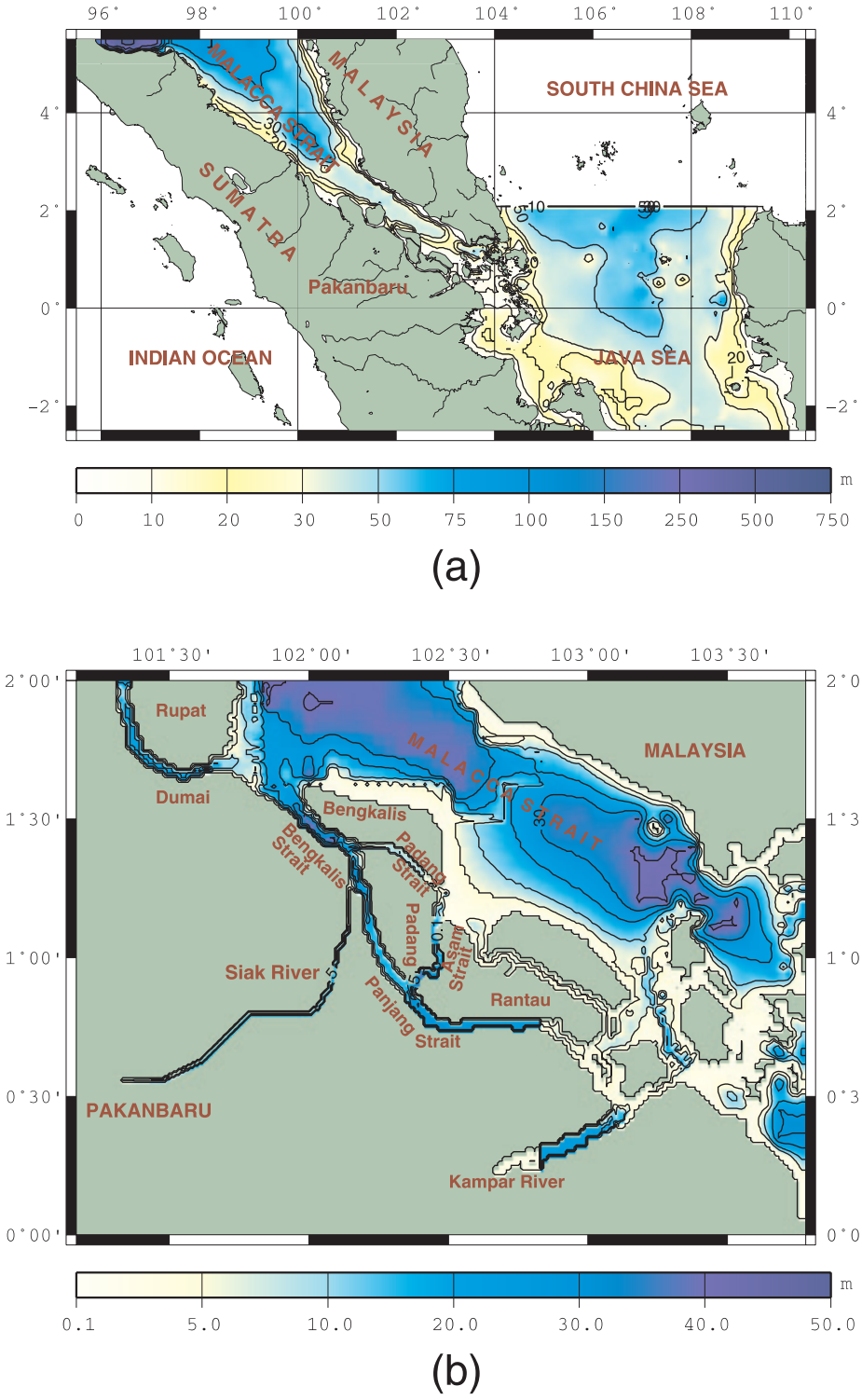

Figure 1: (a) Large model area bathymetry of Java Sea and Malacca Strait and (b) detailed model area of Riau Waters.

The depth of the Malacca Strait around the Riau Islands is shallower than 50 metres (see Figure 1b). The water masses are influenced by the Indian Ocean in the northern part and Java Sea in the south-eastern part. Generally, in the Malacca Strait, the water mass flow is directed towards the Indian Ocean which is strongly related to the sea level gradient in this strait (Wyrtki, 1961).

During the northeast monsoon, the absolute dynamic topography obtained from AVISO Data (2006) in the Andaman Sea, north of the Malacca Strait, is lower than in the Java and South China Seas in the south-eastern part. Therefore, the sea surface currents show the strongest flow towards the Indian Ocean through the Malacca Strait during this season. During the southeast monsoon the dynamic topography is nearly reversed. Nevertheless the sea surface currents still flow towards the Indian Ocean through the Malacca Strait mainly due to the south-easterly surface winds during this monsoon phase.

The geographic and oceanographic conditions around the Siak river estuary are quite complex; therefore to understand the characteristics of the ocean dynamics, a number of numerical simulations have been performed. These simulations should help us to understand in more detail the dynamical processes in this estuary including their impact on the dispersion of matter. In this way, the study can also support decision makers for environmental and land use planning as well as coastal zone management.

Model Description

General Description of HAMSOM

Circulation Model

The circulation model applied in this study is a modified version of the HAMSOM shelf sea model developed by Backhaus (1985). It is a three-dimensional, baroclinic shallow water equation model. Additionally, the equation of state for sea water (Fofonoff and Millard, 1983) and the transport equations for temperature and salinity are employed. The modifications with respect to Backhaus mainly concern the transport equation for temperature and salinity and the formulation of the vertical eddy viscosity. The latter is parameterized using a method developed by Kochergin (1987). In this turbulence closure scheme the vertical eddy viscosity A_v is dependent on the vertical velocity gradient and on the stability of the water column.

$$A_{Iv} = \left(c_{ML} \cdot h_{ML}\right)^2 \cdot \sqrt{\left(\frac{\partial u}{\partial z}\right)^2 + \left(\frac{\partial v}{\partial z}\right)^2 + \frac{1}{S_M}\frac{g}{\rho}\frac{\partial \rho}{\partial z}} \cdot \quad (1)$$

where h_{ML} is the thickness of the mixed layer, c_{ML} a free constant set by Kochergin to $c_{ml} = 0.05$ and S_M is known as the turbulent Schmidt-Prandtl number. The vertical diffusion coefficients A_{Mv} are calculated by: $A_{Mv} = A_{Iv} / S_M$. Further details about the implementation into HAMSOM as well as a validation of the turbulence closure scheme can be found in Pohlmann (1996a).

Numerical Scheme

The differential equations are solved on an Arakawa-C grid. In order to minimize problems arising from longer time-steps, moreover, a rotational matrix is applied for the Coriolis term, guaranteeing a second order accuracy in time. The most detailed overview about the rotation of the Coriolis term and the other numerical formulations are described in Backhaus (1985). The use of longer time-steps is possible since these terms that limit the time-step most severely are treated implicitly. Investigation of the stability criteria shows that it is necessary to have an implicit formulation for vertical shear stress and diffusion terms as well as for terms determining the surface gravity waves, namely the barotropic pressure and the vertically integrated continuity equation that leads to the prognostic equation for the sea surface elevation. All the other terms are formulated explicitly. This also concerns the advective terms in the momentum equation and in the transport equation for temperature and salinity. Sub-scale processes have been parameterized by a horizontal turbulent exchange coefficient of 250 m^2/s as well in the large-scale as in the meso-scale model. This relatively high value is also appropriate also for the meso-scale model since the applied Arakawa J7 algorithm is less diffusive than other second order schemes (Arakawa and Lamb, 1977). Because the free surface waves and the vertical diffusion are treated implicitly, only the explicit formulation of advection can cause limitations of the time-step. But since typical values of the advection velocity are of the order of O (1 m/s) for the spatial scales under consideration the limiting Courant number (Roache, 1985) does not restrict the time step too rigorously.

The high resolution of the model was only possible because the model code was optimized in order to give a good performance on the NEC-SX6 computer of the German Climate Computing Centre (Pohlmann, 2006). This optimization consists of two steps. First, a vectorisation of the model code was performed by loop-switching. Secondly, the parallelisation of the code was

done by means of the domain splitting method, where the model domain is divided into a number of sub-domains in accordance with the number of available processors. The relevant information is exchanged normally every time-step between these sub-domains in particular along the bordering grid points using the MPI (Message Passing Interface) library (www-unix.mcs.anl.gov/mpi).

General Forcing and Boundary Conditions

At the closed lateral boundaries a semi-slip and zero flux condition is applied. Contrarily, at the open boundaries the sea surface elevation is prescribed and a zero gradient condition for the transports is used, which together form a stable boundary condition for the hydrodynamical model parameters. At open boundaries under inflow conditions temperature and salinity values are prescribed, while for outflow conditions a Sommerfeld radiation condition is applied (Orlanski, 1976). At closed boundaries river inflow is simulated by introducing temperature and salinity changes at the respective input grid cells.

At the sea bottom the quadratic stress law is applied and at the sea surface fluxes of momentum, heat and fresh water are calculated by means of bulk formulae from meteorological parameters: 10 m wind speed, sea surface pressure, 2 m air temperature, sea surface temperature, 2 m relative humidity, total cloud cover and total precipitation. The bulk formula for incoming solar radiation was taken from the COHERENS model (Luyten et al., 1999) whereas the outgoing long-wave radiation was calculated according to Fung et al. (1984). The sensible and latent heat flux parameterisation were obtained from Kondo (1975). This set of bulk formulae turned out to give the most reasonable results for the Indonesian waters. It has to be noted that the realistic determination of the latter three fluxes can only be performed in a coupled mode with the help of the hydrodynamical model, since otherwise it is not possible to provide the required actual sea surface temperatures, that influences as well the sensible as the latent heat flux.

Model Setup

As a first step, HAMSOM had been adopted to a larger area reaching from 2.5°S to 5.5°N and 95.5°to 110.5°E, covering the Malacca Strait and the western part of the Java Sea (see insert in Figure 1a). This area is divided into 361 × 193 grid cells horizontally with a spatial resolution of 2.5 minutes (about 4.625 km); it has 17 layers of increasing thickness in the vertical direction: 5 m in the first 10 layers, and 10, 20, 20, 50, 100, 250, and 300 m for the subsequent layers, respectively. The time step used in this simulation is 30 minutes covering a simulation period of 5.5 years (from January 2001 to May 2006).

The major tidal constituent in Malacca Strait is semidiurnal (Wrytki, 1960 and Chen et al., 2005). Therefore, to analyze the seasonal variation in the Riau seawaters the model uses only the M_2 constituent (Zahel, 2000), seven parameters of 6-hourly atmospheric data, i.e., 2 m air temperature, 10 m surface wind (two components), specific humidity, surface pressure, cloud cover, precipitation, from the National Center Environmental Prediction (NCEP/NCAR) (Kalnay et al., 1996) and temperature and salinity data from the World Ocean Atlas 2001 (Conkright et al., 2002) to force and initialise the model.

A nested model strategy is applied is this study. For this purpose a second small-scale model was set-up, covering the vicinity of the Siak river estuary from 0° to 2°N and 101°10′E to 103°47′E with 315 × 241 grid cells. The horizontal resolution is 0.5′ (approx. 0.93 km) and in the vertical the water body is subdivided into nine layers which have each a thickness of 5 m up to the bottom at 45 m depth. Boundary values are taken from the large-scale model, namely the sea surface elevation and temperature as well as salinity data are prescribed along the open boundaries (Figure 1b).

The forcing and initialisation of the small-scale model was performed analogously to the large-scale model with NCEP/NCAR and World Ocean Atlas data. Additionally, along the first 98 km of the Siak River from Pakanbaru to the estuary the salinity is set to 0.2 psu, whereas for the last 2 km, data observed during an own measuring campaign in 2004 are prescribed. Moreover, in the small-scale model the influence of the freshwater discharge from rivers is considered.

General Description of the Transport Model

In principle it is possible to employ two different types of dispersion models, i.e., Eulerian or Lagrangian models. Both types have their advantages and disadvantages. The Eulerian model is more suitable for the simulation of widespread pollutants, whereas Lagrangian models are mainly used to trace single releases of a more localised character.

In this paper only the results from an Eulerian type dispersion model will be presented. The basis of this model is the three-dimensional transport equation for conservative substances which is formulated on a fixed three-dimension numerical grid. The parameters provided

by the circulation model are the three-dimensional circulation pattern to describe the advective transport and the vertical diffusion coefficient which indicate the strength of diffusive processes. Due to scaling arguments horizontal advection could be neglected.

Numerically the advection is solved by an explicit component up-stream scheme, while the vertical diffusion is treated implicitly in order to be able to use a larger time-step. The spatial grid is identical to that one of the circulation model. By this means no information is lost due to an interpolation of the forcing data from the circulation to the transport model. For the transport model a time-step of 30 minutes has been chosen.

Simulation Set-up of the Transport Model

After running the HAMSOM circulation model on the small-scale grid for the Riau Waters a transport model has been applied to perform the following dispersion scenarios:

1. Dispersion simulation of constant and continuous sources for more than five years of simulation time with daily currents taken as forcing. This simulation is used to observe the spreading of pollutants from the Siak River estuary, for which an arbitrary concentration of 100 mg/l was chosen. As an initialisation the concentration of the ambient water was set to 1 mg/l at the beginning of the simulation.
2. Dispersion simulation of an instantaneous release at the first day of each month. These dispersion simulations are performed with daily current fields covering always a one month period. This simulation is conducted for a source at the Siak River mouth, only for the year 2005.

Model Validation

In order to validate the hydrodynamical model results the information from Feliatra (2002), Gin et al. (2000) and the satellite AVHRR from NOAA have been employed.

Based on the former measurement on 11 March-7 April 2001 north of Bengkalis (Feliatra, 2002) in the estuary of the Batan Tengah River (1°30′ - 1°35′N and 102°15′ - 102°20′E), the temperature and salinity in this location are ranging between 28-30°C and 26-30 psu, respectively. From the simulation results, it can be inferred that the temperature and salinity in the same area on 11 March-7 April 2001 lies between 28-31 °C and 28-30 psu. Gin et al. (2000) explained the dynamics of the Singapore Strait and wrote that the water temperature and salinity around the Singapore Strait, based on observations in December 1996 until November 1999, are about 28.3-31.2°C and 28.7-32.2 psu, respectively. In agreement with these findings, the simulation results during the year 2001 at the same location show a temperature and salinity of 28-31.5°C and 28-30 psu. Thus it can be concluded that in general the simulation results provide good quantitative agreement with observations.

In order to provide a more detailled view of the model skill the simulation results have also been compared with monthly sea surface temperature (SST) data from the NOAA AVHRR satellite (Figure 2). In general the average SST from the model simulations is in good agreement with observational data during March and October 2004, and January and August 2005. However, this agreement is larger for the year 2004 compared to 2005. Unfortunately the cloud cover during those periods makes satellite observations impossible for certain locations (indicated by blank areas in Figure 2). Hence the comparisons can only be performed for selected locations, i.e. in October 2004 the SST from simulation is similar to the satellite data around Riau seawaters and north Malacca Strait, respectively 30°C and 29.2°C.

From the simulation it can be shown that the mean SST during January 2005 (figure not shown) is less than 28.5°C, lower than the mean SST in August (with more than 30°C) at the same year. From the NOAA AVHRR data it can be concluded that the SST lower than 27.5°C is transported into the Java Sea from the South China Sea during the northeast monsoon. Altogether it can be concluded that observed and simulated pattern are in a reasonable agreement. This is also true for the absolute values. Maximum differences in general do not exceed 1°C, which is acceptable taking into account the coarse resolution of the atmospheric forcing data.

Dynamical Conditions of the Southern Malacca Strait

Riau is located in the Malacca Strait, between the Indian Ocean in the north-northwest and the Java Sea in the southeast. Based on its location, the dynamical conditions of Riau waters are influenced by both seas.

In January, representing the northeast monsoon, the surface current from the South China Sea flows in south-eastward direction into the Java Sea (Figure 3a). Part of these water masses turn to the northwest entering the Malacca Strait because the sea level in the Java Sea is higher than in the Indian Ocean, as indicated by the anomalies described in the introduction. By this mechanism the warm and low saline water from the Java Sea is transported into the Malacca Strait.

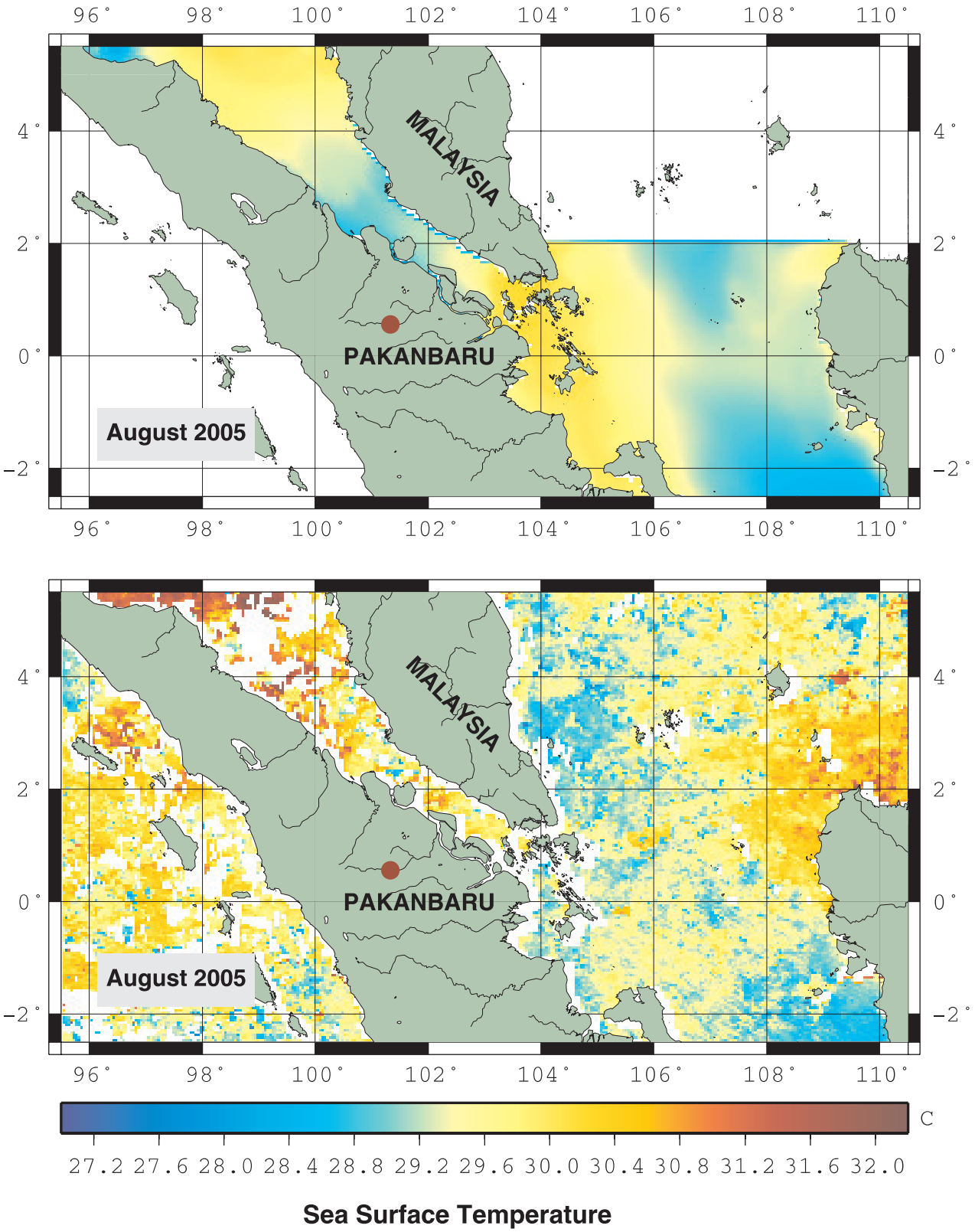

Figure 2: Sea Surface Temperature in the Malacca Strait in August 2005 from HAMSOM Result (upper) and NOAA AVHRR (bottom).

During the southeast monsoon, represented by August 2005, the gradient of the sea level anomaly is reversed. It is now slightly higher in the Malacca Strait compared to the Java Sea. Nevertheless, the sea surface currents still flow into the Malacca Strait from the Java Sea (Figure 3b). The main reason is the monsoonal winds, which predominantly blow from the southeast during this monsoon phase.

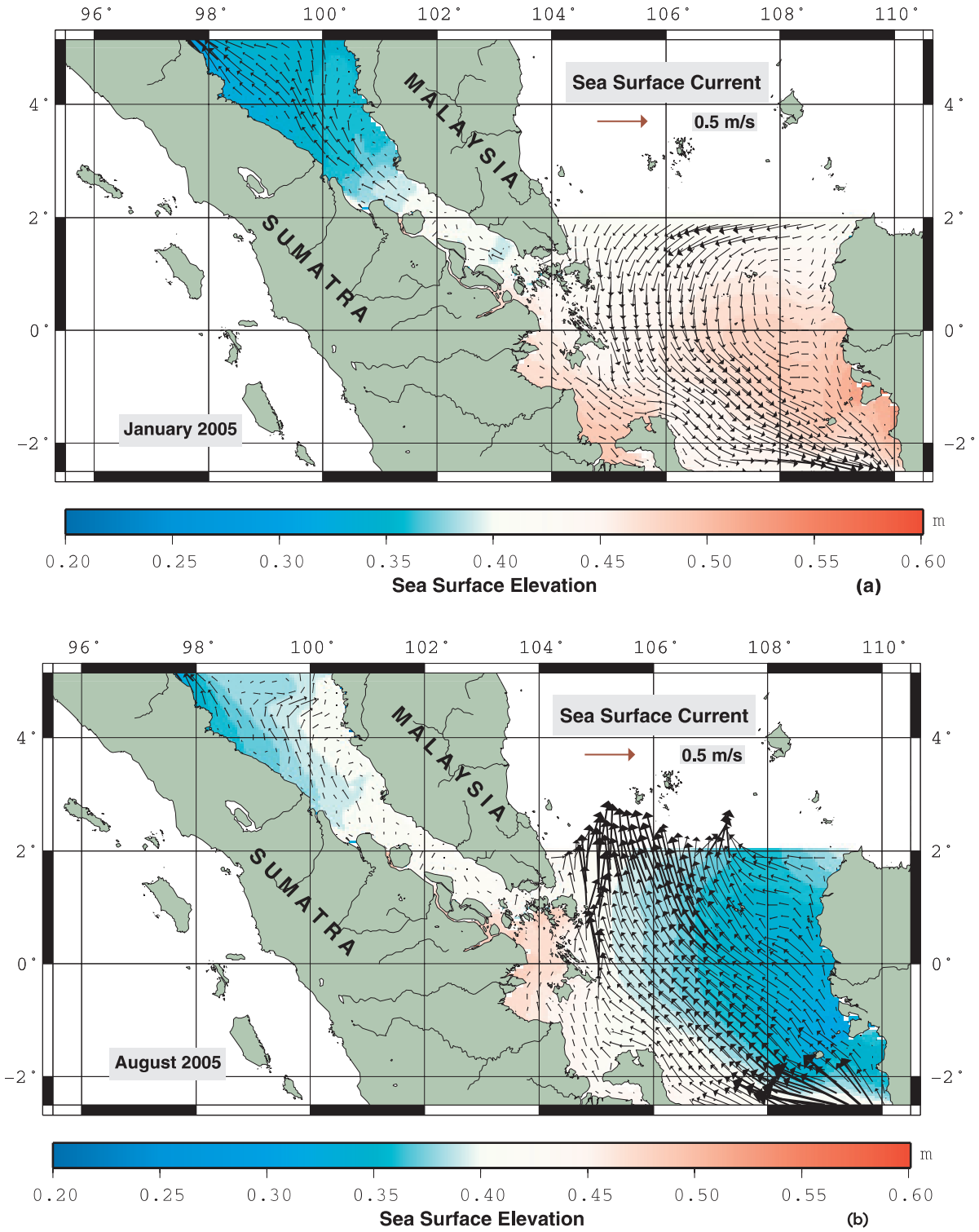

Figure 3: Mean Sea Surface Current of the Malacca Strait (a) in January 2005 and (b) in August 2005.

Dynamic Conditions of the Riau Waters

The small-scale distribution of the sea surface currents as well as the temperature and salinity of the Riau waters in August 2005 are presented in Figures 4 and 5. Warm and low saline water masses (Figure 5) from the Java Sea are transported northward to the Malacca Strait with the transport in August (during the southeast monsoon) being stronger than in January (during the northeast monsoon). In January in the centre of the Malacca Strait, water masses from the Java Sea flow predominantly northward but also are showing a loop current in the vicinity of the Singapore Strait.

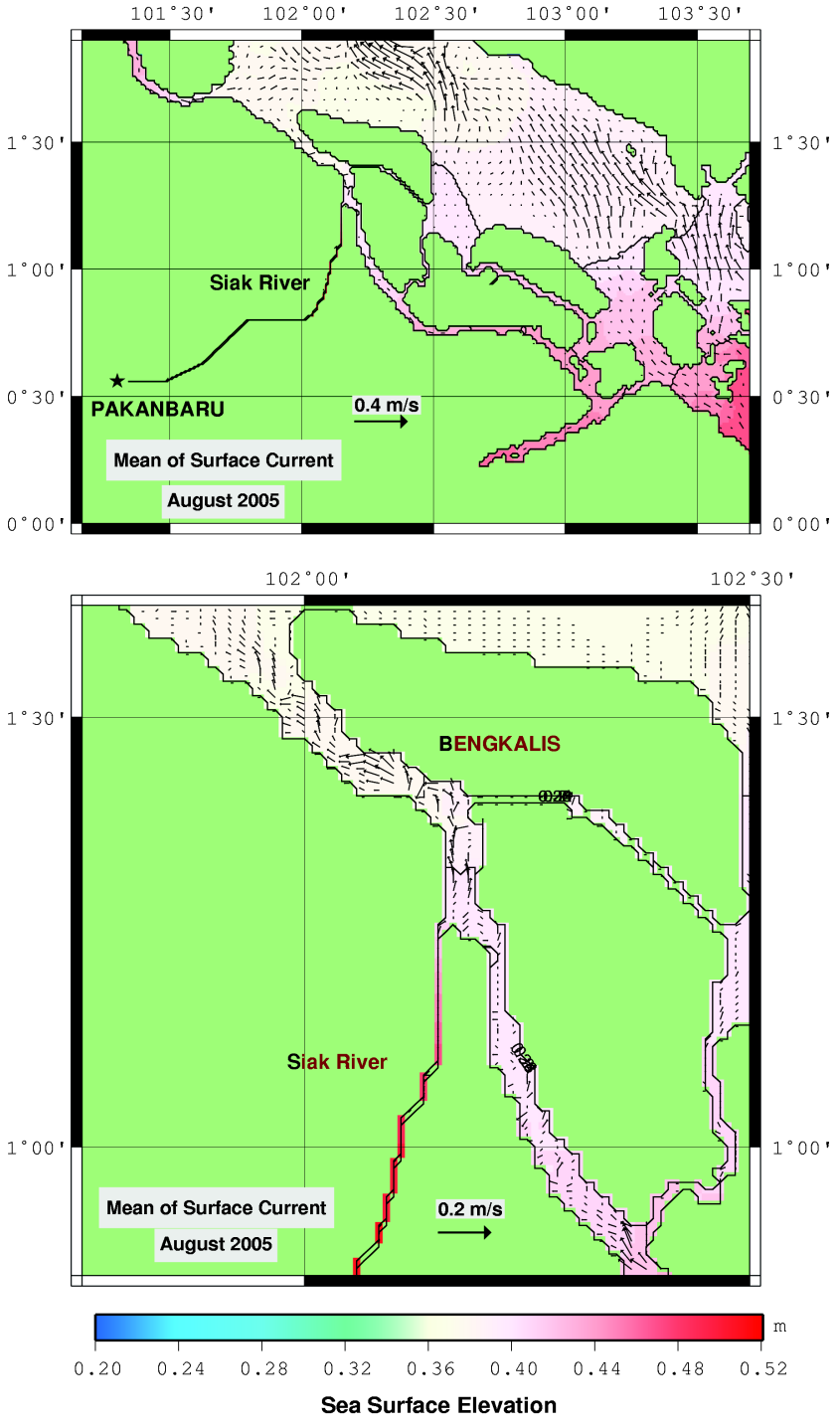

Figure 4: Mean Sea Surface Currents in the Riau waters in August 2005.

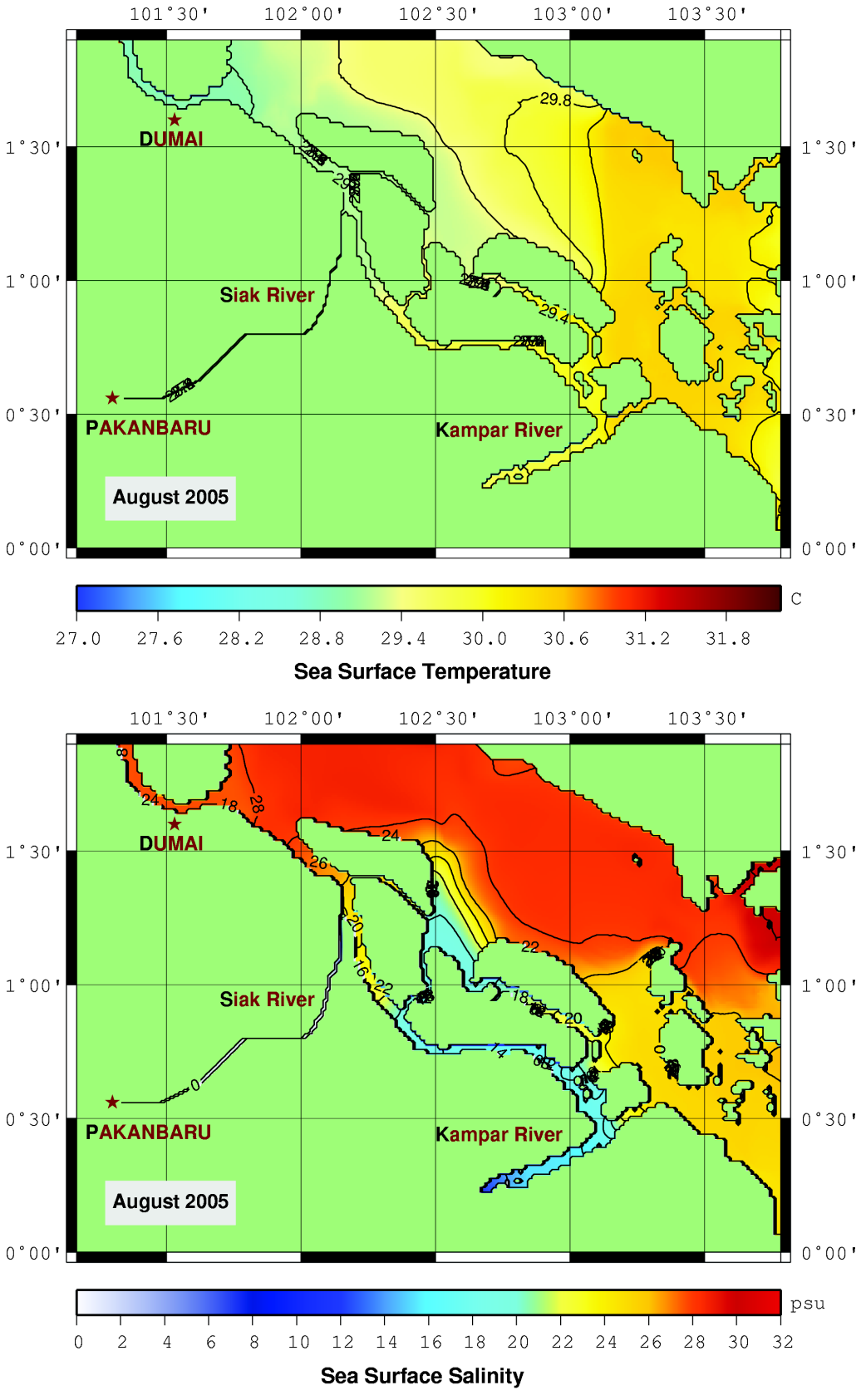

Figure 5: Mean Sea Surface Temperature (top) and Salinity (bottom) in the Riau waters and the adjacent Malacca Strait in August 2005.

As shown in Figure 4, at the Siak river mouth the water is transported dominantly northward almost constantly over the entire years. During the northeast monsoon a rainy season exists and therefore the discharge from the rivers is strong enough and influences the surface currents, whereas the southeast current originating from the Java Sea is as well strong enough. However due to the south-easterly surface winds during this monsoon phase, the sea surface current flow still northward, although the discharge from rivers is small during the southeast monsoon.

The monthly SST in the Malacca Strait is about 27.5-29°C in January and increases to 29-30°C in August in the south-eastern part (Figure 5, top). The increase of the SST during the southeast monsoon in August is caused by the influence of warm water from the Java Sea which flows to the Malacca Strait, while the influence of cold water from the Indian Ocean to the Malacca Strait is not dominant. Nevertheless, the Indian Ocean water mass with higher salinities (more than 29 psu) reaches the north of Bengkalis Island. Around the Padang and Rantau Islands, the water masses show significantly lower salinities of 24 to 26 psu.

Distribution of Pollutants

Continuously Source

At first, a continuously pollutant source at the mouth of the Siak River (100 mg/l) is simulated. Arbitrarily 100 mg/l is assumed to make up 100% of pollutant concentration which is released from 1 January 2001 until 31 May 2006 and transported by daily current provided by the circulation model. After one year of simulation, most of the pollutants have been transported northward to the Malacca Strait. In general the pollutants are transported and dispersed northward. This can be explained by dominantly northward currents as already discussed in an earlier section.

Parts of the pollutants, which move northward towards the Malacca Strait, are transported through the Bengkalis Strait. Moreover, the simulation results show that pollutants can also be transported further south but brought back to the Bengkalis Strait due to the dominant northward current.

During the northeast monsoon, i.e., the rainy season, pollutants are transported to the Malacca Strait only showing relatively low concentrations. High concentrations are only found in the Siak river estuary and along the Bengkalis Strait (see Figures 6a and 6b for conditions in January and March, respectively). At the end of this monsoon phase, in May, the pollutants are transported to the northern entrance of the Bengkalis Strait and still showing high concentrations along the Bengkalis Strait. Meanwhile, during the transition from the southeast to the northeast monsoon in September and October, the weaker northward surface current causes the pollutants to concentrate north and east Bengkalis Island. However, the highest concentrations are found along the Bengkalis Strait in November (beginning of the rainy season).

Results from the transport model show that the spreading of the plume from the Siak river mouth is in good agreement with data from satellite (see Figures 7a and 7b). In analogy to the observed plume from the estuary of the Siak River also the simulated plume is transported to the north through the Bengkalis Strait. However, in both seasons observations show that a minor part of the plume enters the Malacca Strait through the smaller Padang Strait south of Bengkalis Island. The same phenomenon could also be reproduced by the transport simulation. Some discrepancies between model results and observations like the high plume concentrations in the Rupat Channel can be explained by the effect of additional sources which have not been considered in the transport simulation. Also observed high plume concentration south of the Siak River mouth must be attributed to the impact of the Kampar River, which has a much stronger load of sediments than the Siak River.

Non-Continuously Source

Secondly, a non-continuous source was simulated. In this case an arbitrary pollutant with concentration of 100 mg/l was released at each first day of the month in the mouth of Siak River. The resulting distribution at the end of the specific month is analysed in order to discuss the influence of monsoon and its variability on the pollutant transport. The simulations were performed for every month from January to December 2005.

The simulation results show that the distributions after one month of dispersion are almost similar for every year. In January, representing the peak of the northeast monsoon, maximum concentrations after one month are less than 2 mg/l or equal to 2% of the input pollutant concentration. Moreover, from January until May the pollutant has reached the central Malacca Strait through the Bengkalis Strait. The maximum concentration becomes higher, about 7 mg/l or 7% of the pollutant input concentration, during the southwest monsoon. The tip of the plume during this time is located around the northern entrance of the Bengkalis Strait. Because of the lower river discharge during the dry season until the beginning of northeast monsoon (July until November),

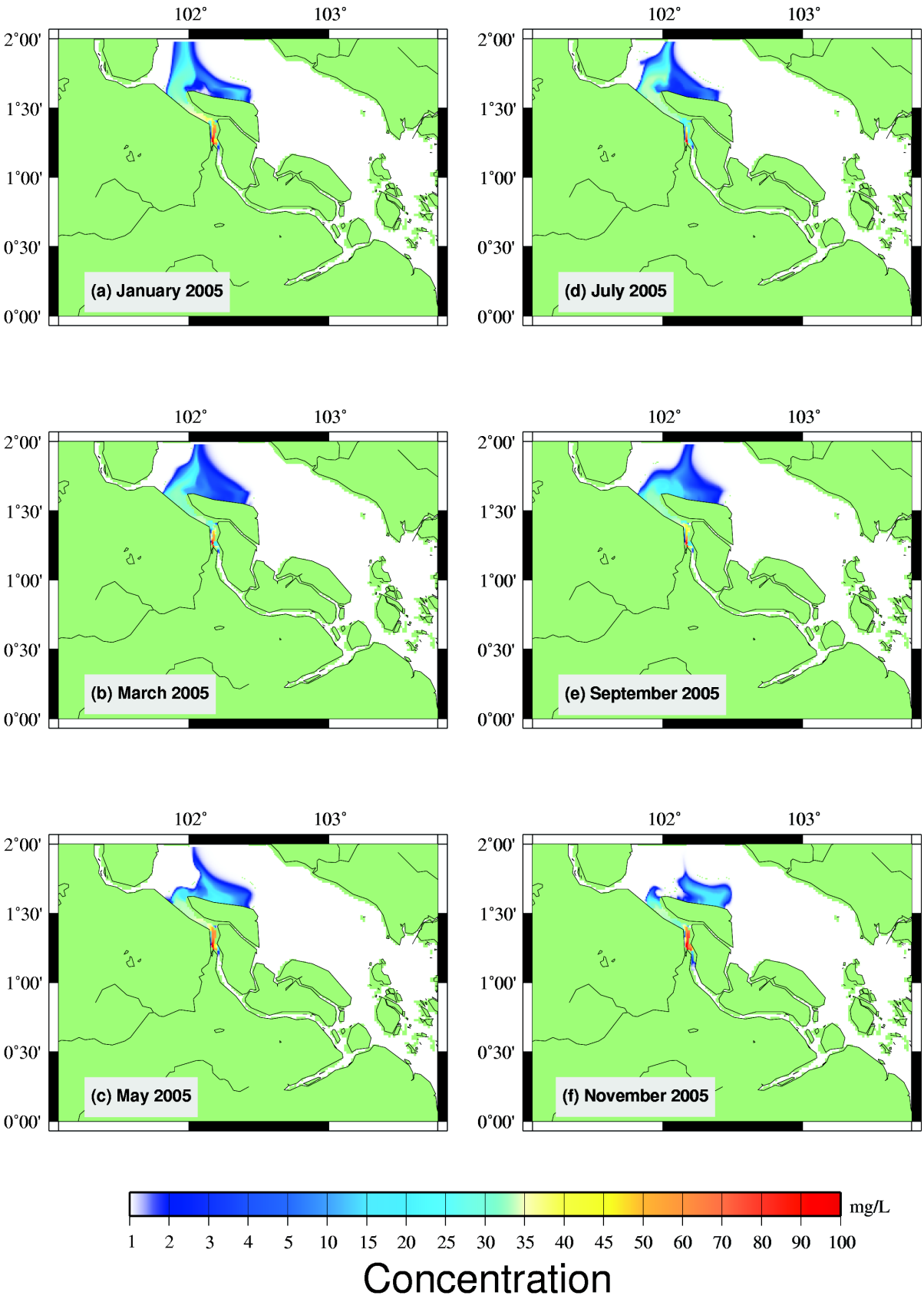

Figure 6: Pollutant concentration from January to November 2005 released continuously from a source at the Siak river mouth starting at 1 January 2001 (a) January, (b) March, (c) May, (d) July, (e) September, and (f) November.

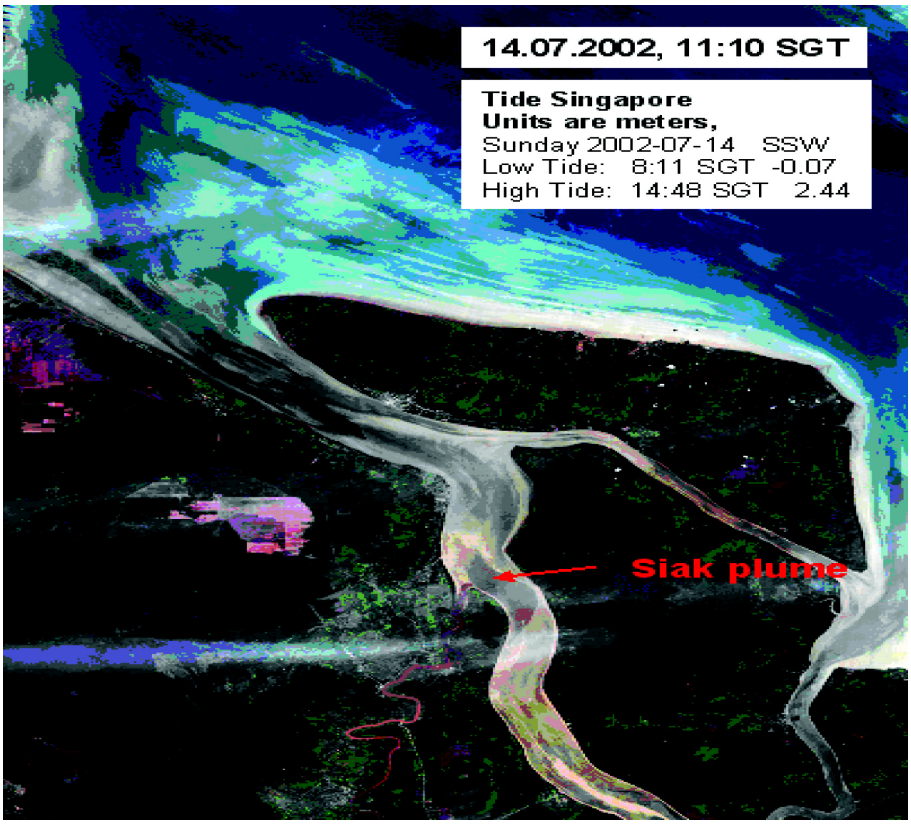

Figure 7(a): Landsat 7 ETM+ scene acquired on 14 July 2002 11:10 SGT showing the Siak River plume during flood tide.

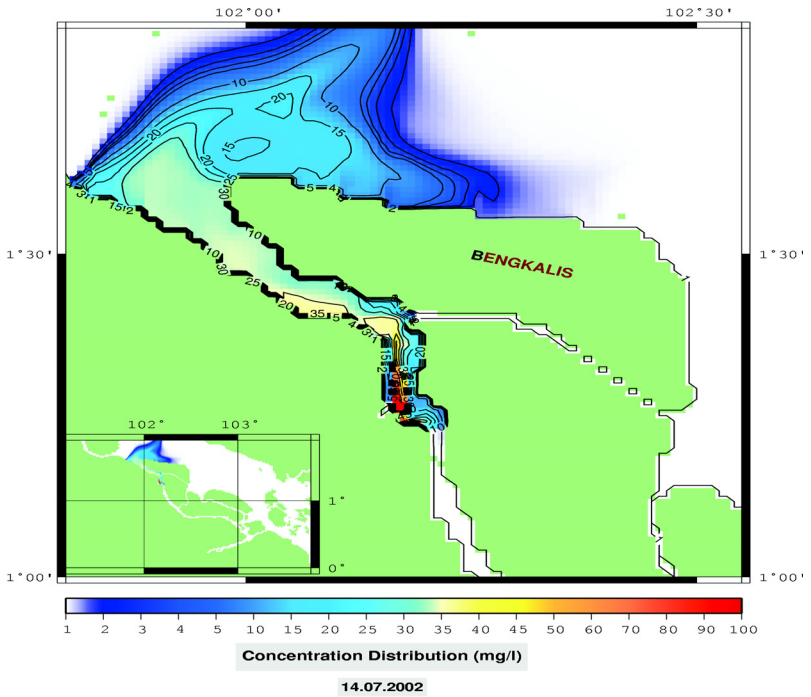

Figure 7 (b): Simulation Results on 14 July 2002 after 1.5 years of continuous release at the Siak river mouth.

the pollutant accumulates near the mouth of Siak River estuary. In contrast, during the northeast monsoon, when the river discharge peaks, the pollutant is transported further to the north reaching the central Malacca Strait as in January.

Conclusion

Several conclusions could be drawn from the above investigations. Firstly, it could be demonstrated that the HAMSOM circulation model is able to reproduce the hydrodynamical conditions in the Riau waters reasonably well. The same is true for the dispersion model. The resulting concentration patterns of substances released at the Siak river mouth are in good agreement with satellite observations.

Secondly, the hydrodynamical simulations prove that the sea level difference between the Java Sea and Indian Ocean causes a predominantly northward flow in the Malacca Strait. Therefore the seawater properties of Java Sea with low salinity are dominating in the southeastern part of the Malacca Strait.

Thirdly, the transport model simulation shows that substances released at the Siak river mouth in general is transported to the north through the Bengkalis into the Malacca Strait. However, a minor part of the Siak river water is transported through the Padang Strait south of Bengkalis Island.

Finally, this dispersion simulation indicates that the longest residence times for substances released at the Siak River mouth occur during the northeast monsoon (in January). After one month of dispersion the maximum concentration found in the Bengkalis Strait still exhibits up to 6-7% of the initial concentration released at the starting day.

Acknowledgement

We would like to thank Herbert Siegel from the Institute of Baltic Sea Research for kindly providing the satellite images. The research was funded by the Federal German Ministry for Education, Research, Science and Technology (BMBF) under grant number 03F0392D.

References

Arakawa, A. and V.R. Lamb (1977). Computational design of the basic dynamical processes of the UCLA general circulation model. *Methods Computational Physics*, **17:** 173-265.

AVISO (2006). Ssalto/Duacs User Handbook: (M)SLA and (M)ADT Near-Real Time and Delayed Time Products. SALP-MU-P-EA-21065-CLS, 1rev4 of the 31 January 2006.

Backhaus, J.O. (1983). A semi-implicit scheme for the shallow water equations for application to shelf sea modelling. *Continent. Shelf Res.*, **2:** 243-254.

Backhaus, J.O. (1985). A Three-Dimensional Model for the Simulation of Shelf Sea Dynamics. *Dt. Hydrogr. Z.*, **38:** 165-187.

Conkright, M.E., Locarnini, R.A., Garcia, H.E., O'Brien, T.D., Boyer, T.P., Stephens, C. and J.I. Antonov (2002). World Ocean Atlas 2001: Objective Analyses, Data Statistics, and Figures, *CD-ROM Documentation*, National Oceanographic Data Center, Silver Spring, MD, 17 pp.

Gin, Karina Yew-Hoong, Lin, X. and S. Zhang (2000). Dynamics and size structure of phytoplankton in the coastal waters of Singapore. *J. of Plankton Research*, **22 (8):** 1465-1484.

Feliatra, Sebaran Bakteri (2002). *Escherichia coli* Di Perairan Muara Sungai Batan Tengah Bengkalis Riau. *J. Natur Indonesia*, **4 (2):** 179-181 (Indonesian).

Fofonoff, N.P. and R.C. Millard Jr. (1983). Algorithms for computation of fundamental properties of sea water. UNESCO Technical Papers in Marine Science, 44.

Fung, I.Y., Harrison, D.E. and A.A. Lacis (1984). On the variability of the net longwave radiation at the ocean surface. *Rev. Geophys.*, **22:** 177-193.

Kalnay, E., Kanamitsu, M., Kistler, R., Collins, W., Deaven, D., Gandin, L., Iredell, M., Saha, S., White, G., Woollen, J., Zhu, Y., Chelliah, M., Ebisuzaki, W., Higgins, W., Janowiak, J., Mo, K.C., Ropelewski, C., Wang, J., Leetmaa, A., Reynolds, R., Jenne R. and D. Joseph (1996). The NCEP/NCAR 40-Year Reanalysis Project. *Bulletin of the American Meteorological Society*, **77 (3):** 437-471.

Kochergin, V.P. (1987) Three-dimensional prognostic models. *In:* Three-dimensional coastal ocean models, N. S. Heaps (ed). Washington, D.C.: American Geophysical Union (Coastal and Estuarine Science 4), pp. 201-208.

Kondo, J. (1975). Air-Sea bulk transfer coefficients in diabatic conditions. *Boundary-Layer Met.*, **9:** 91-112.

Luyten, P.J., Jones, J.E., Proctor, R., Tabor, A., Tett., P., and K. Wild-Allen (1999). COHERENS - A Coupled Hydrodynamical-Ecological Model for Regional and Shelf Seas: User Documentation**.** MUMM Report, Management Unit of the Mathematical Models of the North Sea, 914 p.

Nedi, S. (1999). Kajian Kualitas Air Sungai Siak di Kotamadya Pakanbaru dan Kecamatan Siak Kabupaten Bengkalis. *J. Natur Indonesia*, **1 (1):** 39-43.

Orlanski, I. (1976). A Simple Boundary Condition for Unbounded Hyperbolic Flows. *J. Computat. Phys.*, **21:** 251-269.

Pohlmann, T. (1987). A Three Dimensional Circulation Model of the South China Sea. *In:* Three-Dimensional Models of

Marine and Estuarine Dynamics, J.C.J. Nihoul and B.M. Jamart (eds). Elsevier Science Publishers B.V. Amsterdam.

Pohlmann, T. (1996a) Predicting the thermocline in a circulation model of the North Sea. Part I: Model description, calibration, and verification. *Cont. Shelf Res.*, **16:** 131-146.

Pohlmann, T. (1996b). Calculating the development of the thermal vertical stratification in the North Sea with a three-dimensional circulation model**.** *Continental Shelf Research*, **16 (2):** 163-194.

Pohlmann, T. (2006). A meso-scale model of the central and southern North Sea: Consequences of an improved resolution**.** In press. *Continental Shelf Research.*

Roache, P.J. (1985) Computational fluid dynamics. Hermosa Publishers, New Mexico, U.S.A., 446 p.

Roache, P.J. (1982). On Artificial Viscosity**.** *J. of Computational Physics* **10:** 169-184.

Saunders, P., Coward, A.C. and B.A. de Cuevas. Circulation of the Pacific Ocean seen in a global ocean model (OCCAM). *J. Geophys. Res.*, **104:** 18281-18299.

Wyrtki, K. (1961). Scientific Results of Marine Investigations of the South China Sea and the Gulf of Thailand 1959-1961, Naga Report, Vol. 2, The University of California.

Zahel, W., Gavinko, J.H. and U. Seiler (2000). Angular Momentum and Energy Budget of a Global Ocean Tide with Data Assimilation. GEOS, Ensenada, **20 (4):** 400-413.